The Presence and Absence of Agostic Electrostatic Si−H···M Interactions in [M{$Me_2Si(H)N$-*t*-Bu}] (M = Li, $Mg_{1/2}$) Species

Bernd Goldfuss,† Paul von Ragué Schleyer,* Sandra Handschuh, Frank Hampel, and Walter Bauer

Institut für Organische Chemie der Universität Erlangen-Nürnberg, Henkestrasse 42, D-91054 Erlangen, Germany

Received July 30, 1997[⊗]

Agostic Si−H···Li contacts (i.e. significantly less than ∼3.0 Å) are not present in the solvent-free X-ray structure of $[Li\{Me_2Si(H)N\text{-}t\text{-}Bu\}]_3$; shorter (*t*-Bu)$CH_3$···Li distances (∼2.8 Å) are observed instead. The situation in solution is different. While the $^1H-^6Li$ HOESY spectrum of [Li{$Me_2Si(H)N$-*t*-Bu}] in toluene at −80 °C evidently detects the same trimeric species (lacking Si−H···Li interactions, but with short (*t*-Bu)CH_3···Li contacts), two major species with strong Si−H···Li interactions also are present. In the Li−HN−SiH_3 computational model system, Si−H···Li interactions are favored energetically and result in increased Si−H distances and decreased Si−H frequencies. Agostic Si−H···metal contacts in the solid state are found in the X-ray crystal structure of $[Mg_2\{Me_2Si(H)N\text{-}t\text{-}Bu\}_4]$, where $Li^{"+"}$ is replaced by the more highly charged $Mg^{"2+"}$. The two short agostic Si−H···Mg interactions (2.2, 2.5 Å) which result also are shown by the two low ν(Si−H) frequencies (2040, 1880 cm^{-1}) in the IR spectrum (Nujol mull) of $[Mg_2\{Me_2Si(H)N\text{-}t\text{-}Bu\}_4]$.

Introduction

Agostic interactions[1] are frequently regarded as "frozen intermediate" models of C−H, or Si−H σ-bond activation processes.[2] Oxidative additions of C−H or Si−H σ-bonds by metal complex moieties ML_n are key catalytic steps in hydrocarbon activation[3] or in hydrosilylation-[4] and silane σ-bond metathesis[5] reactions (Scheme 1).[2]

Recently, we studied the electrostatic contribution to metal−σ(C−C)-cyclopropane,[6] metal−π(C≡C)-acetylene,[7] and metal−thiophene[8] interactions. Due to the direction and the enhanced polarity of the $Si^{\delta+}-H^{\delta-}$ bond,[9,10] electrostatics should play an important role in Si−H···M bonding. As electrostatics dominate in organolithium bonding,[9] Si−H···$Li^{(+)}$ agostic interactions should provide good assessments for the electrostatic component in Si−H···M arrangements.

In 1986, Schleyer and Clark predicted computationally that the "inverted" structure of LiH_3Si (**1**) was more stable than the "tetrahedral" (also C_{3v}) alternative.[11] Later, inverted $SiH_3^-Na^+$ moieties (Na−H = 2.52−2.67 Å) were found in the X-ray crystal structure of $[Na_8(O_3C_5H_{11})_6(SiH_3)_2]$ and were shown to be favored electrostatically.[12] Short Si−H···Li distances (Li−H = 1.89−1.91 Å) are apparent in the X-ray crystal structure of the lithium amide $(Me_3Si)_2NSi(H)[N(Li)SiMe_3]_2$.[13]

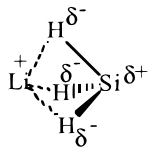

1

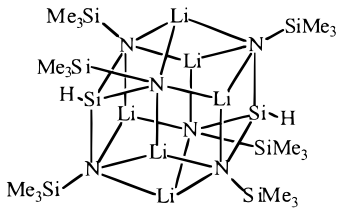

$(2)_2$

Agostic Si−H···Li interactions (Li−H = 1.97−2.32 Å) were found to be responsible for the distortion of the molecular skeleton of MeSi(H)[N(Li)-*t*-Bu]$_2$.[14] However,

† Present address: Department of Chemistry and Biochemistry, University of California, Los Angeles (UCLA), 405 Hilgard Ave., Los Angeles, CA 90095-1569.

⊗ Abstract published in *Advance ACS Abstracts,* December 1, 1997.

(1) Brookhart, M.; Green, M. L. H. *J. Organomet. Chem.* **1983**, *250*, 395.

(2) (a) Schneider, J. J. *Angew. Chem.* **1996**, *108*, 1132; *Angew. Chem., Int. Ed. Engl.* **1996**, *35*, 1068. (b) Schubert, U. *Adv. Organomet. Chem.* **1990**, *30*, 151. (c) Bauer, W.; Schleyer, P. v. R. *J. Am. Chem. Soc.* **1989**, *111*, 7191.

(3) (a) Strout, D. L.; Zaric, S.; Niu, S.; Hall, M. B. *J. Am. Chem. Soc.* **1996**, *118*, 6068. (b) Stahl, S. S.; Labinger, J. A.; Bercaw, J. E. *J. Am. Chem. Soc.* **1996**, *118*, 5961. (c) Arndtsen, B. A.; Bergman, R. G.; Mobley, T. A.; Peterson T. H. *Acc. Chem. Res.* **1995**, *28*, 154. (d) Hofmann, P. In *Organometallics in Organic Synthesis*; de Meijere, A.; tom Dieck, H., Eds.; Springer: Berlin, 1987; p 1.

(4) (a) Tilley, T. D. In *The Chemistry of Organic Silicon Compounds*; Patai, S., Rappoport, Z., Eds.; Wiley: Chichester, U.K., 1989; Vol. II, p 1458. (b) Fryzuk, M. D.; Rosenberg, L.; Rettig, S. J. *Organometallics* **1996**, *15*, 2871. (c) Hofmann, P. In *Silicon Chemistry*; Auner, N., Weis, J., Eds.; VCH: Weinheim, Germany, 1993; p 231. (d) Hofmann, P.; Meier, C.; Hiller, W.; Heckel, M.; Riede, J.; Schmidt, M. U. *J. Organomet. Chem.* **1995**, *490*, 51.

(5) Tilley, T. D. *Acc. Chem. Res.* **1993**, *26*, 22 and references therein.

(6) Goldfuss, B.; Schleyer, P. v. R.; Hampel, F. *J. Am. Chem. Soc.* **1996**, *118*, 12183.

(7) Goldfuss, B.; Schleyer, P. v. R.; Hampel, F. *J. Am. Chem. Soc.* **1997**, *119*, 1072.

(8) Goldfuss, B.; Schleyer, P. v. R.; Hampel, F. *Organometallics*, in press.

(9) The Allred−Rochow electronegativities of H and Si are 2.2 and 1.74, respectively: (a) Apeloig, Y. In *The Chemistry of Organic Silicon Compounds*; Patai, S., Rappoport, Z., Eds.; Wiley: Chichester, U.K., 1989. (b) Pawlenko, S. *Organosilicon Chemistry*; de Gruyter: Berlin, 1986.

(10) (a) Streitwieser, A.; Bachrach, S. M.; Dorigo, A.; Schleyer, P. v. R. In *Lithium Chemistry*; Sapse, A.-M., Schleyer, P. v. R., Eds.; Wiley: New York, 1995. (b) Lambert, C.; Schleyer, P. v. R. *Angew. Chem.* **1994**, *106*, 1187; *Angew. Chem., Int. Ed. Engl.* **1994**, *33*, 1129. (c) Lambert, C.; Schleyer, P. v. R. In *Houben-Weyl Methods of Organic Chemistry*, 4th ed.; Thieme: Stuttgart, Germany, 1993; Vol. E19d, p 1.

(11) Schleyer, P. v. R.; Clark, T. *J. Chem. Soc., Chem. Commun.* **1986**, 1371.

(12) Pritzkow, H.; Lobreyer, T.; Sundermeyer, W.; Hommes, N. J. R. v. E.; Schleyer, P. v. R. *Angew. Chem.* **1994**, *106*, 221; *Angew. Chem., Int. Ed. Engl.* **1994**, *33*, 126.

(13) Veith, M.; Zimmer, M.; Kosse, P. *Chem. Ber.* **1994**, *127*, 2099.

S0276-7333(97)00656-0 CCC: $14.00

Scheme 1. Oxidative Si−H Addition as the Key Step in *σ*-Bond Metathesis and Hydrosilylation Reactions

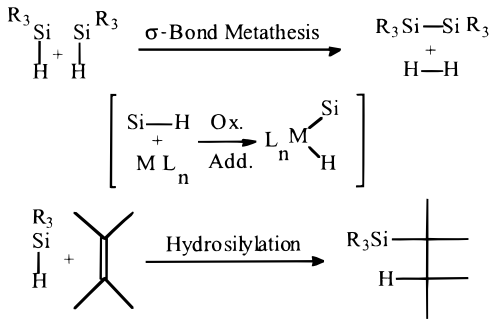

no Si−H···Li coordination was detected in solution (^{1}H, ^{6}Li NMR) or in the solid state (X-ray analysis) for the $HSi(Me_3SiNLi)_3$ dimer (**2**).[15]

Agostic η^2-Si−H···M coordination was found in molybdenum,[16] titanium,[17] and ruthenium[18] complexes. The **3-H** > **3-I** > **3-Br** > **3-Cl** > **3-F** agostic Si−H···Zr

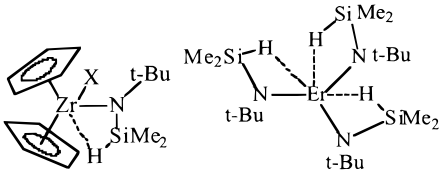

3-X

X = H, F, Cl, Br, I

4

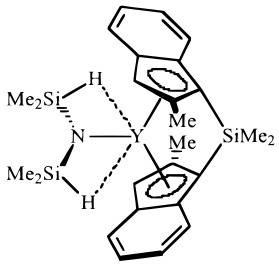

5

interaction order was evaluated by means of NMR criteria (upfield $\delta(^{29}Si,^1H)$ and small $^1J_{SiH}$) as well as the decrease in ν(SiH), the stretching vibration frequencies.[19] Agostic Si−H···Zr interactions are evident from X-ray crystal structures of **3-H** and **3-Cl**.[19] The "trisagostic" Si−H···Er character in **4** was suggested to be responsible for the high vapor pressure and the low melting point of **4**.[20] Two Si−H···Y contacts are apparent in **5**.[21] Recently, Sekiguchi et al. observed a SiH−

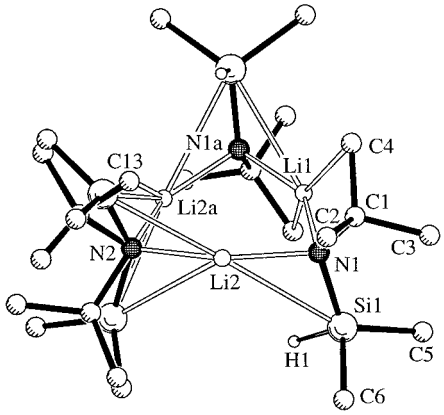

Figure 1. Representation of the X-ray crystal structure of (**6-Li**)$_3$. The hydrogen atoms of Si_2 and the methyl groups are omitted. For bond distances and angles see Table 1.

Li agostic interaction in (1,1,2,2-tetrakis(dimethylsilyl)-1,2-ethanediyl)dilithium−bis(diethyl ether).[22]

To assess the electrostatic contribution of Si−H···M interactions involving the $\{Me_2Si(H)N\text{-}t\text{-}Bu\}^-$ ligand, we have now studied lithium (**6-Li**) and magnesium (**6-Mg**) derivatives of **6-H** by experimental (e.g. X-ray diffraction) methods. In addition, computations on model compounds are provided for comparison.

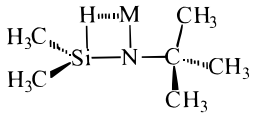

M = H (**6-H**),
Li (**6-Li**),
$Mg_{1/2}$ (**6-Mg**)

Results and Discussion

X-ray Single-Crystal Analysis and ^{1}H-^{6}Li-HOESY of [Li{Me_2Si(H)N-*t*-Bu}]. The X-ray crystal structure of [Li{Me_2Si(H)N-*t*-Bu}] (**6-Li**) reveals a trimeric solvent-free aggregate (Figure 1). Disorder appears for the $SiMe_2$ and *t*-Bu moieties at N(2) (shown in Figure 1) as well as for the *t*-Bu groups at N(1) and N(1a). As in the X-ray crystal structure of $[(Me_3Si)_2NLi]_3$,[23] **6-Li** adopts a planar $(LiN)_3$ ring with perpendicular Si(H)-Me_2 and *t*-Bu moieties (Figure 1). The H−Si bonds are not oriented toward lithiums but bisect the LiNLi angles (Li(1)−N(1)−Si(1)−H(1) = 48.1°, Li(2)−N(1)−Si(1)−H(1) = 48.2°; Table 1). These Si(H)Me_2 arrangements result in long Si−H···Li distances (H(1)−Li(1) = 2.99 Å, H(1)−Li(2) = 2.98 Å). In contrast, the (*t*-Bu)-CH_3 groups tend to coordinate the lithiums (C(4)−Li(1) = 2.78 Å, C(13)−Li(2a) = 2.75 Å; Figure 1, Table 1). No lithium affinity of the (Si)CH_3 groups is apparent (C(5)−Li(1), C(6)−Li(2) > 3.5 Å; Table 1).

However, the structure of the species in solution is different and there is evidence for Si−H···Li interactions. While the magnitudes of scalar $^1J_{H-Si}$ coupling constants as well as of δ_H and δ_{Si} only give indirect evidence for short Si−H···M distances in solution,[19]

(14) Becker, G.; Abele, S.; Dautel, J.; Motz, G.; Schwarz, W. In *Organosilicon Chemistry II*; Auner, N., Weis, J., Eds.; VCH: Weinheim, Germany, 1996.
(15) Kosse, P.; Popowski, E.; Veith, M.; Huch, V. *Chem. Ber.* **1994**, *127*, 2103.
(16) (a) Luo, X.-L.; Kubas, G. J.; Bryan, J. C.; Burns, C. J.; Unkefer, C. J. *J. Am. Chem. Soc.* **1994**, *116*, 10312. (b) Fan, M.-F.; Jia, G.; Lin, Z. *J. Am. Chem. Soc.* **1996**, *118*, 9915.
(17) Spaltenstein, E.; Palma, P.; Kreutzer, K. A.; Willoughby, C. A.; Davis, W. M.; Buchwald, S. L. *J. Am. Chem. Soc.* **1994**, *116*, 10308.
(18) Delpech, F.; Sabo-Etienne, S.; Chaudret, B.; Daran, J.-C. *J. Am. Chem. Soc.* **1997**, *119*, 3167.
(19) Procopio, L. J.; Carroll, P. J.; Berry, D. H. *J. Am. Chem. Soc.* **1994**, *116*, 177.
(20) Rees, W. S., Jr.; Just, O.; Schumann, H.; Weinmann, R. *Angew. Chem.* **1996**, *108*, 481; *Angew. Chem., Int. Ed. Engl.* **1996**, *35*, 419.
(21) Herrmann, W. A.; Eppinger, J.; Spiegler, M.; Runte, O.; Anwander, R. *Organometallics* **1997**, *16*, 1813.
(22) Sekiguchi, A.; Ichinohe, M.; Takahasi, M.; Kabuto, C.; Sakurai, H. *Angew. Chem.* **1997**, *109*, 1577; *Angew. Chem., Int. Ed. Engl.* **1997**, *36*, 1533.
(23) (a) Mootz, D.; Zinnius, A.; Bötcher, B. *Angew. Chem.* **1969**, *81*, 398; *Angew. Chem., Int. Ed. Engl.* **1969**, *8*, 378. (b) Rogers, R. D.; Atwood, J. L.; Grüning, R. *J. Organomet. Chem.* **1978**, *157*, 229.

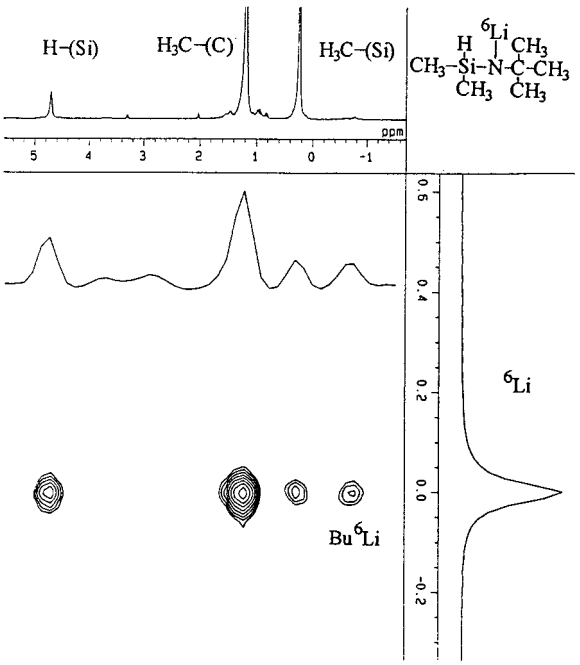

Figure 2. ^{1}H−^{6}Li HOESY contour plot of **6-^{6}Li** (toluene-d_8, +25 °C, c = 2.0 M, mixing time 2.0 s). δ(^{6}Li) is arbitrarily set to zero. Cross peaks between ^{6}Li and the ^{1}H nuclei are shown.

Table 1. Bond Distances (Å) and Bond and Torsion Angles (deg) in the X-ray Crystal Structure of [Li{Me$_2$Si(H)N-*t*-Bu}]$_3$ (Figure 1)

Li(1)−N(1)	1.945(5)	H(1)−Li(1)	2.987(7)
Li(2)−N(1)	1.955(9)	H(1)−Li(2)	2.981(7)
Li(2)−N(2)	1.957(9)	C(4)−Li(1)	2.778(10)
Li(1)−Si(1)	2.943(2)	C(2)−Li(2)	2.939(10)
Li(1)−C(5)	3.658(5)	Li(2)−C(6)	3.726(5)
Li(2)−Si(1)	2.929(9)	C(13)−Li(2)	3.674(20)
Li(2)−Si(2)	2.734(10)	C(13)−Li(2a)	2.747(20)

Li(1)−N(1)−Si(1)	108.0(2)	Li(1)−N(1)−Si(1)−H(1)	48.1(4)
Li(2)−N(1)−Si(1)	106.8(4)	Li(2)−N(1)−Si(1)−H(1)	48.2(4)
Li(1)−N(1)−C(1)−C(4)	16.9(5)	Li(2)−N(1)−C(1)−C(2)	39.7(5)

^{1}H−^{6}Li-HOESY (heteronuclear overhauser effect spectroscopy) detects short Li···H distances directly through space by dipolar relaxation processes.[24] The ^{1}H−^{6}Li-HOESY spectrum of **6-^{6}Li** at +25 °C in toluene-d_8 exhibits one ^{6}Li signal with strong cross peaks to H(Si) and to the CH_3(*t*-Bu) groups as well as weaker cross signals to the CH_3(Si) moieties (Figure 2). Cooling the **6-^{6}Li** sample down to −80 °C results in three ^{6}Li peaks (Figure 3); these are consistent with three different ^{6}Li locations, e.g. in three different aggregates or forms of **6-^{6}Li**. These are resolved in the ^{1}H−^{6}Li-HOESY spectrum at −80 °C (Figure 3), where the central and the upfield ^{6}Li peaks exhibit cross signals to H(Si), to CH_3-(*t*-Bu), and to CH_3(Si). These two species with Si−H··· Li contacts are the major components in solution.

However, the third species with the most downfield δ(^{6}Li) value only shows contacts to the *t*-Bu groups and *no* cross signals to H(Si) and CH_3(Si) (Figure 3). This ^{1}H−^{6}Li-HOESY behaviour is consistent with the long Si−H···Li and Si−CH_3···Li distances as well as the short (*t*-Bu)CH_3···Li arrangements in the X-ray crystal structure of **6-Li**. Hence, ^{1}H−^{6}Li-HOESY of this minor species with the most downfield δ(^{6}Li) values (Figure 3) points to a close structural relationship to the solid-state X-ray crystal structure of **6-Li** (Figure 1). These results provide further examples of differences between solid-state and solution structures of lithium compounds.[25]

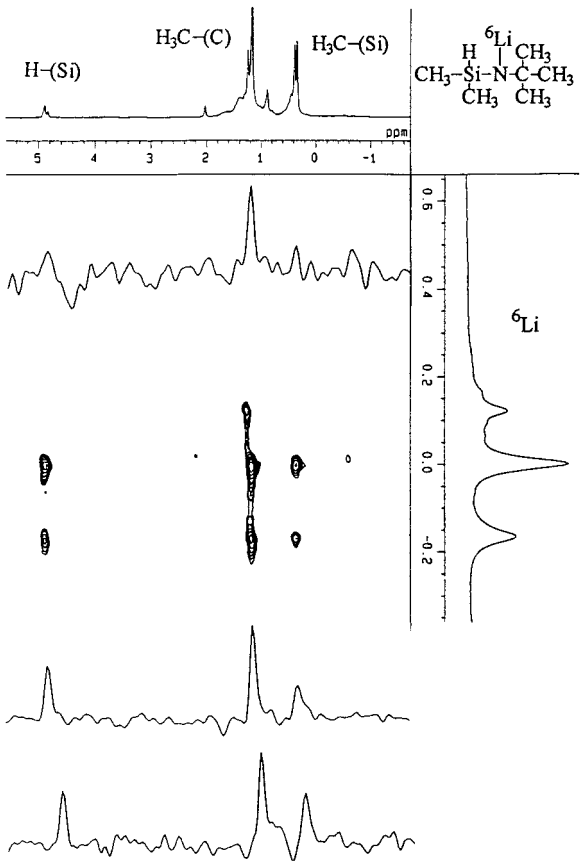

Figure 3. ^{1}H−^{6}Li HOESY contour plot of **6-^{6}Li** (toluene-d_8, −80 °C, c = 2.0 M, mixing time 2.0 s). The central δ(^{6}Li) is arbitrarily set to zero. The three ^{6}Li signals indicate the presence of three distinct species or lithium locations. The δ(^{6}Li) signal at lowest field shows no cross peaks to H(Si) and to CH_3(Si).

Computational Model for Agostic Si−H···Li Interactions. In order to assess the effects of electrostatic Si−H···Li interactions computationally, we optimized H_2NSiH_3 (**7**; C_s, NIMAG = 0) as well as the lithiated species $LiHNSiH_3$ both without Li−H contacts (**7-Li-trans**, C_s, NIMAG = 1) and with Li−H contacts (**7-Li-cis**, C_s, NIMAG = 0; Figure 4, Table 2). Lithiation of the NH_2 group in **7** shortens the N−Si bond length in **7-Li-trans** and results in longer Si−H(1−3) distances and in a smaller H(1)−Si−N angle (Figure 4). These geometrical changes are even more pronounced upon rotation of the LiHN group in **7-Li-trans** to the minimum geometry **7-Li-cis** (Figure 4). The Si−H···Li contact in **7-Li-cis** increases the Si−H(1) bond length and decreases the H(1)−Si−N angle considerably (Figure 4). Due to the attractive Si−H(1)···Li interaction, the **7-Li-cis** conformation is 2.2 kcal/mol more stable than **7-Li-trans** (Table 2).

(24) (a) Bauer, W.; Schleyer, P. v. R. *Magn. Reson. Chem.* **1988**, *26*, 827. (b) Bauer, W.; Clark, T.; Schleyer, P. v. R. *J. Am. Chem. Soc.* **1987**, *109*, 970.

(25) (a) Bauer, W. In *Lithium Chemistry*; Sapse, A.-M., Schleyer, P. v. R., Eds.; Wiley: New York, 1995. (b) Weiss, E. *Angew. Chem.* **1993**, *105*, 1565; *Angew. Chem., Int. Ed. Engl.* **1993**, *32*, 1501. (c) Setzer, W. N.; Schleyer, P. v. R. *Adv. Organomet. Chem.* **1985**, *24*, 353. (d) Günther, H.; Moskau, D.; Bast, P.; Schmalz, D. *Angew. Chem.* **1987**, *99*, 1242; *Angew. Chem., Int. Ed. Engl.* **1987**, *26*, 1212.

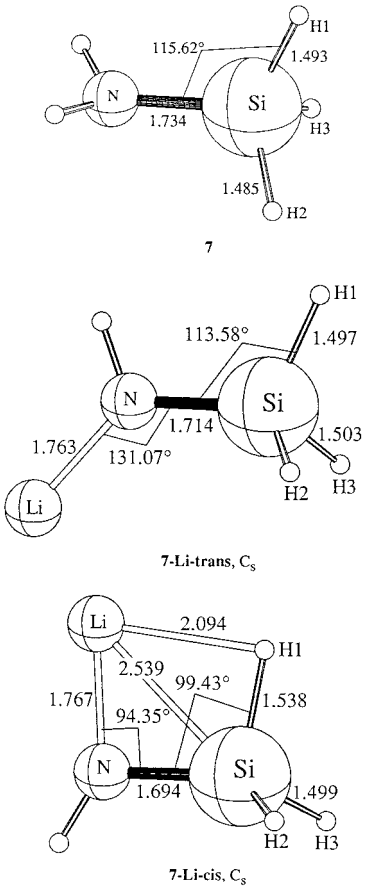

Figure 4. RB3LYP/6-311+G** optimized geometries (Table 2) of H_2NSiH_3 (**7**, C_s, NIMAG = 0), $LiHNSiH_3$ (**7-Li-trans**, C_s, NIMAG = 1; **7-Li-cis**, C_s, NIMAG = 0).

Table 2. Computed Energies,[a] Si−H Stretching Frequencies ω,[a] NPA Charges q,[b] and ^{1}H Chemical Shifts δ[c]

	7 (C_s)	**7-Li-trans** (C_s)	**7-Li-cis** (C_s)
total energy (au)	−347.319 18	−354.253 47	−354.257 93
ZPE (kcal/mol) (NIMAG)	31.50 (0)	24.82 (1)	25.39 (0)
rel energy (kcal/mol)		+2.23	0
ω(H(1)−Si (cm^{-1})	2180	2162	1955
q(Li) (au)		+0.964	+0.949
q(H(1)) (au)	−0.204	−0.211	−0.295
q(H(2,3)) (au)	−0.181	−0.229	−0.215
δ(H(1))	+5.44	+5.47	+5.05
δ(H(2,3))	+5.19	+5.61	+5.96

[a] RB3LYP/6-311+G** optimizations and frequency computations. [b] Natural population analysis.[31] [c] B3LYP/6-311+G**-GIAO computations;[32] the δ values are relative to the computed absolute chemical shielding of H (32.29) in TMS.

While the H_2N lithiation affects the Si−H(1) stretching frequency only slightly in **7-Li-trans** (2162 vs 2180 cm^{-1} in **7**), ω(Si−H(1)) is strongly decreased by the Si−H(1)···Li contact in **7-Li-cis** (1955 cm^{-1}; Table 2). The Si−H(1)···Li interaction also increases the negative charge on H(1) and results in a slightly upfield shifted δ^1H(1) value in **7-Li-cis** relative to **7-Li-trans** (Table 2).

X-ray Crystal Structure of [Mg{Me$_2$Si(H)N-*t*-Bu}$_2$]. Although computations show that the (Si)H$^{\delta-}$···Li$^+$ contact in **7-Li-cis** is favored electrostatically (Figure 4, Table 2), no short (Si)H···Li distances are apparent in the X-ray crystal structure of **6-Li** (Figure 1, Table 1). However, we find that replacement of Li$^{"+"}$ with Mg$^{"2+"}$ results in short Si−H$^{\delta-}$···Mg$^{"2+"}$ distances in the solid state, presumably due to increased positive charge on the metal center.[10b,c,26]

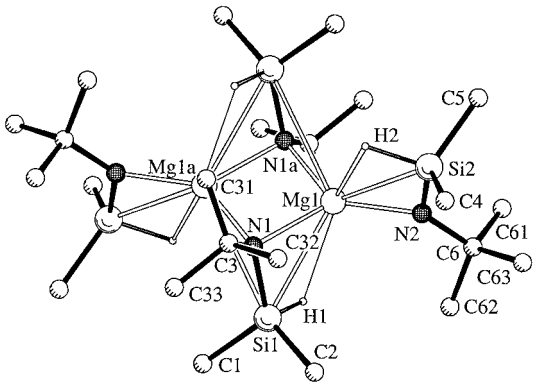

Figure 5. X-ray crystal structure of (**6-Mg**)$_2$. The hydrogen atoms of the methyl groups are omitted. For bond distances and angles see Table 3.

Table 3. Bond Distances (Å) and Bond and Torsion Angles (deg) in the X-ray Crystal Structure of [Mg{Me$_2$Si(H)N-*t*-Bu}$_2$]$_2$ (Figure 5)

Mg(1)−N(1)	2.139(1)	H(1)−Mg(1)	2.495(10)
Mg(1)−N(2)	1.984(2)	H(2)−Mg(1)	2.227(10)
Mg(1)−N(1a)	2.133(1)	C(31)−Mg(1a)	2.984(10)
Mg(1)−Si(1)	2.922(1)	H(1)−Si(1)	1.379(10)
Mg(1)−Si(2)	2.792(1)	H(2)−Si(2)	1.469(10)
Mg(1)−N(2)−Si(2)	98.83(7)	H(1)−Si(1)−N(1)−Mg(1)	26.5
Mg(1)−N(2)−C(6)	136.81(11)	H(2)−Si(2)−N(2)−Mg(1)	0.8
C(3)−N(1)−N(1a)	130.1(1)	C(31)−C(3)−N(1)−Mg(1a)	32.4
Si(1)−N(1)−N(1a)	111.91(14)		

The X-ray crystal structure analysis of [Mg{Me$_2$Si-(H)N-*t*-Bu}$_2$] reveals dimeric aggregation of **6-Mg** (Figure 5). Two distinct amido moieties are apparent, the one bridging between two magnesium centers, the other bonding terminally to the magnesiums. Short Si−H··· Mg contacts are apparent for the bridging (H(1)−Mg(1) = 2.50 Å) and especially for the terminal (H(2)-Mg(1) = 2.23 Å) amido groups (Figure 5, Table 3). These short Si−H···Mg distances are supported by the tilt of the Me_2SiH groups toward the magnesiums (Si(1)−N(1)−N(1a) = 111.9°, Si(2)−N(2)−Mg(1): 98.8°), while the *t*-Bu moieties are bent away from the magnesium centers (C(3)−N(1)−N(1a) = 130.1°, C(6)−N(2)−Mg(1) = 136.8°, Figure 5, Table 3). The nearly perfect coplanarity of the H(2)−Si(2) and the N(2)−Mg(1) bonds (H(2)−Si(2)−N(2)−Mg(1): 0.8°, Figure 5, Table 3) favors short Si−H···Mg distances especially for the terminally bonded amido groups.

In accord with the two distinct Me_2SiH moieties in the X-ray crystal structure of [Mg$_2${Me$_2$Si(H)N-*t*-Bu}$_4$] (Figure 5), two distinct Si−H stretching frequencies are observed in the IR spectrum of **6-Mg**. The lowering of these frequencies (Table 4) can be attributed to Si−H···-Mg interactions, which are weaker in the bridging (*t*-BuN)Me_2SiH groups (slightly reduced ν(Si−H) 2040 cm^{-1}) and stronger in the terminally bonded (*t*-BuN)Me_2-SiH moieties (strongly decreased ν(Si−H) 1880 cm^{-1}).

Conclusions

The reason why agostic electrostatic Si−H···M interactions develop in **6-Mg** rather than in **6-Li** appears to

(26) The partial (NPA) charge on Mg in magnesium amides (e. g. $HMgNMe_2$) is ca. +1.5 au: Goldfuss, B.; Schleyer, P. v. R. Unpublished results.

Table 4. Experimental ν(Si−H) Frequencies (cm^{-1})

compd	ν(Si−H)	compd	ν(Si−H)
3-H, 3-F	1912, 1998[a]	**6-H**	2120,[b] 2111,[c] 2107[a]
4	1858[c]	**6-Li**	2060[d]
5	1804[e]	**6-Mg**	2040, 1880[d]

[a] C_6H_6 solution.[19] [b] Neat (this work). [c] C_6D_6 solution.[20] [d] Nujol mull (this work). [e] Reference 21.

be due to the higher partial charge of $Mg^{"2+"}$ vs $Li^{"1+"}$. In general, we conclude that the metal charges are crucial in determining the formation of electrostatic Si−H···M arrangements, which are for higher positive metal charges (e.g. $Mg^{"2+"}$) more readily established than for lower positive charges (e.g. $Li^{"1+"}$).

Experimental Section

The experiments were carried out under an argon atmosphere by using standard Schlenk as well as needle/septum techniques. The solvents were distilled from sodium/benzophenone and stored on Na/Pb alloy. Chlorodimethylsilane (Me_2SiHCl), *tert*-butylamine (*t*-$BuNH_2$) and dibutylmagnesium ($MgBu_2$, 1.0 M in heptane) were purchased from Acros. A hexane solution of ^{6}Li-enriched *n*-Bu^{6}Li was prepared as described by Seebach et al.[27] The NMR spectra were recorded on a JEOL GX 400 spectrometer (^{1}H, 400 MHz; ^{13}C, 100.6 MHz; ^{6}Li, 58.9 MHz). ^{1}H and ^{13}C spectra were referenced to the solvent signals (toluene). IR spectra were determined as neat samples or as Nujol mulls between NaCl disks on a Perkin-Elmer 1420 spectrometer. Mass spectral data were obtained on a Varian MAT 311A spectrometer and elemental analyses (C, H) on a Heraeus micro automaton. The X-ray crystal data were collected with a Nonius Mach3 diffractometer using ω/θ-scans. The structures were solved by direct methods using SHELXTL Plus 4.11. The parameters were refined with all data by full-matrix least squares on F^2 using SHELXL93 (G. M. Sheldrick, Göttingen, Germany, 1993). Non-hydrogen atoms were refined anisotropically. The (Si)H atoms were localized and refined free isotropically; the hydrogen atoms of methyl groups were fixed in idealized positions using a riding model. R1= $\Sigma|F_o - F_c|/\Sigma F_o$ and wR2 = $\Sigma w|(F_o^2 - F_c^2)^2|/\Sigma(w(F_o^2)^2)^{0.5}$. Further details are available on request from the Director of the Cambridge Crystallographic Data Center, Lensfield Road, GB-Cambridge CB2 1EW, by U.K. quoting the journal citation.

Me_2Si(H)N(H)-*t*-Bu (6-H) was prepared according to the literature procedure.[28] **[Li{Me_2Si(H)N-*t*-Bu}] (6-Li).** To a stirred solution of 0.24 g (1.8 mmol) of **6-H** was added 1.1 mL of 1.6 M *n*-BuLi at 0 °C. After it was stirred at room temperature for 5 min, the solution was frozen with liquid nitrogen (−196 °C), brought to room temperature for 15 s, and then cooled to −20 °C, yielding colorless crystals of **6-Li**: ^{1}H NMR (toluene-d_8, +25 °C) δ 4.70 (m, *H*Si), 1.20 (s, CH_3 *t*-Bu), 0.10 (d, (CH_3)$_2$Si); ^{13}C{^{1}H} NMR (toluene-d_8, +25 °C) δ 52.55 (C, *t*-Bu), 37.31 (*C*H_3, *t*-Bu), 5.27 (*C*H_3, Si); ^{6}Li NMR (toluene-d_6, +25 °C) δ(^{6}Li) singlet; δ(^{6}Li) was arbitrarily set to zero; ^{6}Li NMR (toluene-d_6, −80 °C) δ +0.12, 0.00, −0.16; IR (Nujol mull, cm^{-1}) 2060 (ν(Si−H)); MS (**6-^{7}Li**, EI, 70 eV, 90 °C) *m/e* 411 [Li{Me_2Si(H)N-*t*-Bu}]$_3$. Anal. Calcd for $C_6H_{16}LiNSi$: C, 52.6, H, 11.7. Found: C, 51.8; H, 12.5.

X-ray crystal data for (**6-Li**)$_3$: M_r = 137.23; monoclinic; space group *C*2/*c*; a = 17.910(3) Å, b = 10.410(2) Å, c = 15.829(2) Å, β = 102.08(2)°; V = 2885.9(7) Å^3; D_{calc} = 0.948 Mg m^{-3}; Z = 12; F(000) = 912; Mo Kα (λ = 0.710 73 Å); T = 193(2) K; crystal size 0.20 × 0.20 × 0.20 mm; 4° < 2θ < 54°. There were 3232 reflections collected, of which 3134 were independent and 1127 had $I > 2\sigma(I)$; there were 171 refined parameters. The final R values were R1 = 0.0839 ($I > 2\sigma(I)$) and wR2 = 0.131 51 (all data). GOF = 1.008; the largest peak and hole were 0.286 and −0.293 e Å^{-3}, respectively.

The *t*-Bu and $SiMe_2$ moieties in the X-ray crystal structure of **6-Li** are statistically disordered. A refinement in the acentric space group *Cc*, as suggested by a reviewer, was attempted but failed. All data are consistent with *C*2/*c*.

[Mg{Me_2Si(H)N-*t*-Bu}$_2$] (6-Mg). A 0.24 g (1.8 mmol) amount of **6-H** and 1.8 mL of $MgBu_2$ (1.0 M in heptane) were stirred at 25 °C for 3 days. The solution was frozen with liquid nitrogen (−196 °C) and subsequently warmed to room temperature several times. Storing the sample at 4 °C for 6 weeks yielded colorless crystals of **6-Mg**: ^{1}H NMR (toluene-d_8, +25 °C) δ 4.86 (m, *H*Si), 1.46 (s, CH_3 *t*-Bu), 0.40 (d, (CH_3)$_2$Si); ^{13}C-{^{1}H} NMR (toluene-d_8, +25 °C) δ 54.47 (C, *t*-Bu), 37.78 (*C*H_3, *t*-Bu), 5.31 (*C*H_3, Si); IR (Nujol mull, cm^{-1}) 2040, 1880 (ν(Si−H)); MS (EI, 70 eV, 90 °C) *m/e* 569 [Mg_2{Me_2Si(H)N-*t*-Bu}$_4$], 439 [Mg_2{Me_2Si(H)N-*t*-Bu}$_3$], 309 [Mg_2{Me_2Si(H)N-*t*-Bu}$_2$]. Anal. Calcd for $C_{12}H_{32}MgN_2Si_2$: C, 50.7; H, 11.3. Found: C, 49.9; H, 12.1.

X-ray crystal data for (**6-Mg**)$_2$: M_r = 284.89; monoclinic; space group $P2_1/c$; a = 11.371(2) Å, b = 13.497(2) Å, c = 12.168-(3) Å, β = 106.58(2)°; V = 1789.8(5) Å^3; D_{calc} = 1.057 Mg m^{-3}; Z = 4; F(000) = 632; Mo Kα (λ = 0.710 73 Å); T = 173(2) K; crystal size 0.40 × 0.40 × 0.30 mm; 4° < 2θ < 52°. There were 3662 reflections collected, of which 3623 were independent and 2866 had $I > 2\sigma(I)$; there were 282 refined parameters. The final R values were R1 = 0.0319 ($I > 2\sigma(I)$) and wR2 = 0.0922 (all data). GOF = 1.023; the largest peak and hole were 0.364 and −0.206 e Å^{-3}, respectively.

Computational Methods. All theoretical structures were optimized using the gradient techniques implemented in GAUSSIAN 94[29] with Becke's three-parameter hybrid functional incorporating the Lee−Yang−Parr correlation term (Becke3LYP)[30] and the 6-311+G** basis set. The character of the stationary points and the zero-point energy corrections were obtained from analytical frequency calculations. All partial charges are based on the natural population analysis (NPA)[31] of the Becke3LYP electron density. Absolute chemical shieldings were computed with the B3LYP/6-311+G**-GIAO[32] method.

Acknowledgment. This work was supported by the Fonds der Chemischen Industrie (also through a scholarship to B.G.), the Stiftung Volkswagenwerk, and the Deutsche Forschungsgemeinschaft.

Supporting Information Available: Further details on the X-ray crystal structures of **6-Li** and **6-Mg**, including tables of atomic coordinates, bond lengths and angles, and thermal parameters (15 pages). Ordering information is given on any current masthead page.

OM970656+

(27) Seebach, D.; Hässig, R.; Gabriel, J. *Helv. Chim. Acta* **1983**, *66*, 308.

(28) (a) Wiseman, G. H.; Wheeler, D. R.; Seyferth, D. *Organometallics* **1986**, *5*, 146. (b) Jarvie, S. W.; Lewis, D. *J. Chem. Soc.* **1963**, 4758.

(29) Frisch, M. J.; Trucks, G. W.; Schlegel, H. B.; Gill, P. M. W.; Johnson, B. G.; Robb, M. A.; Cheeseman, J. R.; Keith, T.; Petersson, G. A.; Montgomery, J. A.; Raghavachari, K.; Al-Laham, M. A.; Zakrzewski, V. G.; Ortiz, J. V.; Foresman, J. B.; Cioslowski, J.; Stefanov, B. B.; Nanayakkara, A.; Challacombe, M.; Peng, C. Y.; Ayala, P. Y.; Chen, W.; Wong, M. W.; Andres, J. L.; Replogle, E. S.; Gomperts, R.; Martin, R. L.; Fox, D. J.; Binkley, J. S.; Defrees, D. J.; Baker, J.; Stewart, J. P.; Head-Gordon, M.; Gonzalez, C.; Pople, J. A. Gaussian 94, Revision C.3; Gaussian, Inc., Pittsburgh, PA, 1995.

(30) (a) Becke, A. D. *J. Chem. Phys.* **1993**, *98*, 5648. (b) Lee, C.; Yang, W.; Parr, R. G. *Phys. Rev.* **1988**, *B37*, 785.

(31) (a) Reed, A. E.; Curtiss, L. A.; Weinhold, F. *Chem. Rev.* **1988**, *88*, 899. (b) Reed, A. E.; Schleyer, P. v. R. *J. Am. Chem. Soc.* **1990**, *112*, 1434.

(32) (a) Wolinski, R. F. W.; Hilton, F. J.; Pulay, P. *J. Am. Chem. Soc.* **1990**, *112*, 8251. (b) Dodds, J. L.; McWeeney, R.; Sadlej, A. J. *Mol. Phys.* **1980**, *41*, 1419. (c) Ditchfield, R. *Mol. Phys.* **1974**, *27*, 789. (d) McWeeny, R. *Phys. Rev.* **1962**, *126*, 1028. (e) London, F. *J. Phys. Radium* **1937**, *8*, 397.